MODELLING OF PHASE TRANSFORMATIONS IN STEEL WELD METAL

H. K. D. H. Bhadeshia

University of Cambridge
Department of Materials Science and Metallurgy
Pembroke Street, Cambridge CB2 3QZ, U.K.

Abstract

This paper deals with some of the latest issues in the modelling of steel weld microstructures, building on work already published in the open literature. The key factors reviewed include the nature of acicular ferrite (a most desirable phase), the formation of austenite in the heat–affected zone and finally, the tempering reactions in welds which are post–weld heat treated for service at elevated temperatures.

1. INTRODUCTION

The welding process attempts to achieve perfect metallic joints without the thermomechanical processing inherent in the manufacture of wrought steels. This is impossible to achieve in practice but there are many tools which can be exploited on the path to perfection. One of these involves the calculation of microstructure in ferritic steel welds, work which has been documented and reviewed thoroughly [1–8]. The reviews are widely available; their contents are not therefore repeated here. It is the intention here to highlight the very latest developments and difficulties in the modelling of steel weld microstructures.

2. MICROSTRUCTURE

Typical components of the microstructure are listed in Fig. 1, classified into two essential categories: displacive and reconstructive.

TABLE 1: Approximate values of the shear strain s and the dilatational strain δ for a variety of transformation products in steels.

Transformation	s	δ	Morphology
Widmanstätten ferrite, α_w	0.36	0.03	Thin plates
Bainite, α_b	0.22	0.03	Thin plates
Martensite, α'	0.24	0.03	Thin plates
Allotriomorphic α	0	0.03	irregular
Idiomorphic α	0	0.03	equiaxed
Pearlite	0	0.03	irregular

In a displacive transformation, the change in crystal is achieved by a deformation of the parent structure (Table 1). The strain energy due to the deformation can be minimised if the product phase adopts a thin–plate shape during constrained transformation [9]. Consequently, martensite, bainite, acicular ferrite and Widmanstätten ferrite all occur in the

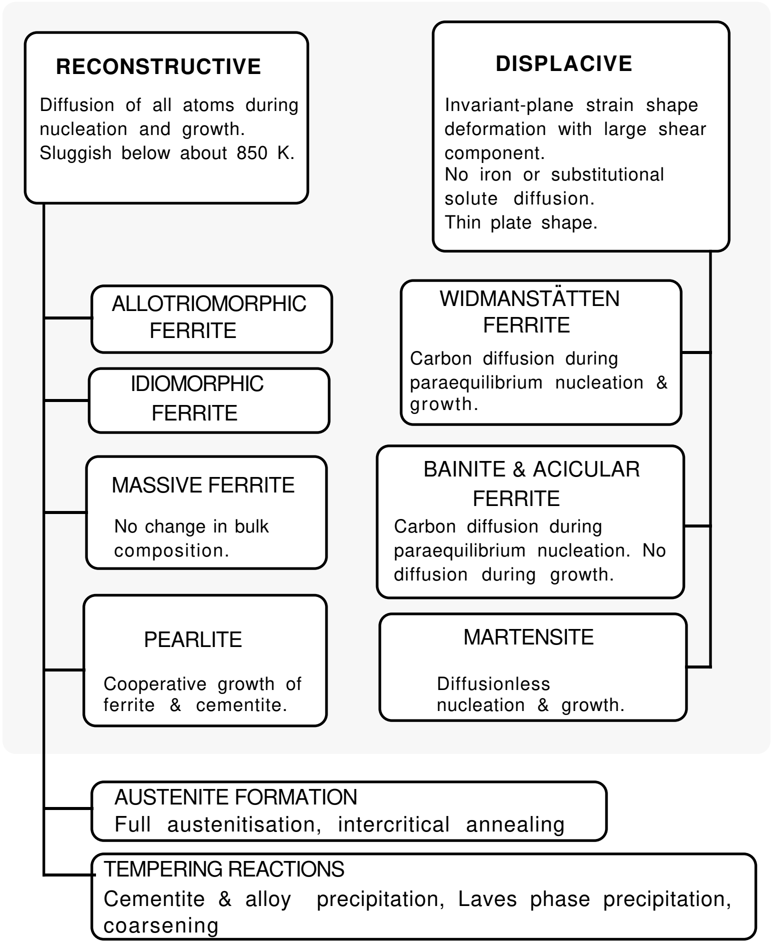

FIGURE 1: Flow chart of the mechanisms of solid–state transformations in steel welds. The shaded region deals with transformation during the cooling of austenite.

form of thin plates. Furthermore, the ratio (Ξ) of iron to substitutional atoms is unaffected since these atoms do not partition at any stage in the formation of the product phase. Interstitial atoms such as carbon and nitrogen may partition without affecting the displacive character of the change in crystal structure. A change in which Ξ remains constant but where carbon achieves equality of chemical potential is known as *paraequilibrium* transformation [10]. Thus, martensitic transformation is completely diffusionless. Bainite, acicular ferrite and Widmanstätten ferrite nucleate by a paraequilibrium mechanism. However, bainite and acicular ferrite grow without diffusion; any excess carbon is then partitioned into the residual austenite or precipitates as carbides. In the case of Widmanstätten ferrite the paraequilibrium state is maintained during both nucleation and growth.

The difference between acicular ferrite and bainite is that the latter generally nucleates at austenite grain surfaces, so that sheaves of identically oriented parallel plates dominate the microstructure. Acicular ferrite, on the other hand, nucleates from tiny nonmetallic inclusions; these plates radiate from the point nucleation sites, giving a less organised microstructure which has a greater resistance to crack propagation. We shall return to this remarkable microstructure in a later discussion.

Reconstructive transformations involve the diffusion of all elements, including iron.

Thus, the only strain that can be generated during the formation of allotriomorphic ferrite, idiomorphic ferrite and pearlite is that associated with the change of density due to transformation. Strain plays a relatively minor role.

Whereas there is a coordinated transfer of at least the iron and substitutional atoms during a displacive transformation, the flow of atoms for a reconstructive reaction is without discipline. As a consequence, the products of reconstructive transformations are not restricted to the austenite grain in which they nucleate. The coordinated displacements associated with martensite *etc.* cannot be sustained across austenite grain boundaries so that martensite plates are confined to the grain in which they nucleate.

The difference between these two mechanisms of transformation is far from academic. For example, because the displacive transformation products fail to cross austenite (γ) grain boundaries, there is a vestige of the γ grain boundary which remains when transformation in completed. This renders the *prior austenite grain boundaries* susceptible to impurity segregation and intergranular embrittlement. This is not the case with reconstructive transformations where the ferrite grows across the austenite grain boundaries, thereby destroying them as impurity segregation sites. This example highlights the fact that a good understanding of phase transformations not only permits the calculation of microstructure but also helps in achieving better mechanical properties. Table 2 shows the detailed information available on each of the major phases found in steel welds; this kind of information is essential before any calculations can be attempted.

3. ACICULAR FERRITE

Of all the phases described above, acicular ferrite remains the most controversial and the most desirable for good mechanical properties.

Acicular ferrite has in three–dimensions the morphology of thin, lenticular plates which nucleate heterogeneously on nonmetallic inclusions. However, some plates may stimulate the nucleation of others, an effect known as autocatalysis.

It has been argued that acicular ferrite and bainite are similar in their transformation mechanisms. Their microstructures differ in detail because bainite sheaves grow as a series of parallel platelets emanating from austenite grain *surfaces*, whereas acicular ferrite platelets nucleate intragranularly at *point* sites so that parallel formations of plates cannot develop. The nucleation site in the latter case is smaller than the ultimate thickness of the plate, so that the inclusion becomes engulfed by the plate of ferrite which it stimulates.

The growth of both bainite and acicular ferrite causes an invariant–plane strain shape deformation with a large shear component. Consequently, plates of acicular ferrite cannot cross austenite grain boundaries, because the coordinated movement of atoms implied by the shape change cannot be sustained across grains in different crystallographic orientations. The lattice of the acicular ferrite is therefore generated by a deformation of the austenite, so that the iron and substitutional solutes are unable to diffuse during the course of transformation. It is not surprising that the concentrations of substitutional alloying elements are unchanged during the growth of acicular ferrite. This has been verified directly using atomic resolution chemical analysis [11].

The deformation which changes the austenite into acicular ferrite occurs on particular planes and directions, so that the ferrite structure and orientation are intimately related to

TABLE 2: Detailed characteristics of martensite (α'), upper and lower bainite (α_{ub}, α_{lb}, acicular ferrite (α_a), allotriomorphic ferrite (α), idiomorphic ferrite (α_i) and pearlite (P). An = indicates consistency with comment, $\neq$ that the comment does not apply and $\otimes$ that the comment sometimes applies.

Comment	α'	α_{lb}	α_{ub}	α_a	α_w	α	α_i	P
Nucleation and growth reaction	=	=	=	=	=	=	=	=
Plate shape	=	=	=	=	=	$\neq$	$\neq$	$\neq$
IPS shape change with large shear	=	=	=	=	=	$\neq$	$\neq$	$\neq$
Diffusionless nucleation	=	$\neq$	$\neq$	$\neq$	$\neq$	$\neq$	$\neq$	$\neq$
Only carbon diffuses during nucleation	$\neq$	=	=	=	=	$\neq$	$\neq$	$\neq$
Reconstructive diffusion during nucleation	$\neq$	$\neq$	$\neq$	$\neq$	$\neq$	=	=	=
Often nucleates intragranularly on defects	=	$\neq$	$\neq$	=	$\neq$	$\neq$	=	$\neq$
Diffusionless growth	=	=	=	=	$\neq$	$\neq$	$\neq$	$\neq$
Reconstructive diffusion during growth	$\neq$	$\neq$	$\neq$	$\neq$	$\neq$	=	=	=
Atomic correspondence (all atoms) during growth	=	=	=	=	$\neq$	$\neq$	$\neq$	$\neq$
Atomic correspondence only for large atoms	=	=	=	=	=	$\neq$	$\neq$	$\neq$
Bulk redistribution of X atoms during growth	$\neq$	$\neq$	$\neq$	$\neq$	$\neq$	$\otimes$	$\otimes$	$\otimes$
Local equilibrium at interface during growth	$\neq$	$\neq$	$\neq$	$\neq$	$\neq$	$\otimes$	$\otimes$	$\otimes$
Local paraequilibrium at interface during growth	$\neq$	$\neq$	$\neq$	$\neq$	=	$\otimes$	$\otimes$	$\neq$
Diffusion of carbon during transformation	$\neq$	$\neq$	$\neq$	$\neq$	=	=	=	=
Carbon diffusion-controlled growth	$\neq$	$\neq$	$\neq$	$\neq$	=	$\otimes$	$\otimes$	$\otimes$
Co-operative growth of ferrite and cementite	$\neq$	$\neq$	$\neq$	$\neq$	$\neq$	$\neq$	$\neq$	=
High dislocation density	=	=	=	=	$\otimes$	$\neq$	$\neq$	$\neq$
Incomplete reaction phenomenon	$\neq$	=	=	=	$\neq$	$\neq$	$\neq$	$\neq$
Necessarily has a glissile interface	=	=	=	=	=	$\neq$	$\neq$	$\neq$
Always has an orientation within the Bain region	=	=	=	=	=	$\neq$	$\neq$	$\neq$
Grows across austenite grain boundaries	$\neq$	$\neq$	$\neq$	$\neq$	$\neq$	=	=	=
High interface mobility at low temperatures	=	=	=	=	=	$\neq$	$\neq$	$\neq$
Displacive transformation mechanism	=	=	=	=	=	$\neq$	$\neq$	$\neq$
Reconstructive transformation mechanism	$\neq$	$\neq$	$\neq$	$\neq$	$\neq$	=	=	=

that of the austenite. It follows that, plates of acicular ferrite, like bainite, must without exception have an orientation relationship with the austenite.

During isothermal transformation, the acicular ferrite reaction stops when the carbon concentration of the remaining austenite makes it impossible to decompose without diffusion. This implies that the plates of acicular ferrite grow supersaturated with carbon, but the excess carbon is shortly afterwards rejected into the remaining austenite. This of course, is the incomplete reaction phenomenon, where the austenite never reaches its equilibrium composition since the reaction stops at the T_0' curve of the phase diagram (Fig. 2). The obvious conclusion is that acicular ferrite cannot form at temperatures above the bainite–start temperature, and this is indeed found to be the case in practice [12].

There are many other correlations which reveal the analogy between acicular ferrite and bainite. For example, the removal of inclusions by vacuum arc melting, without changing

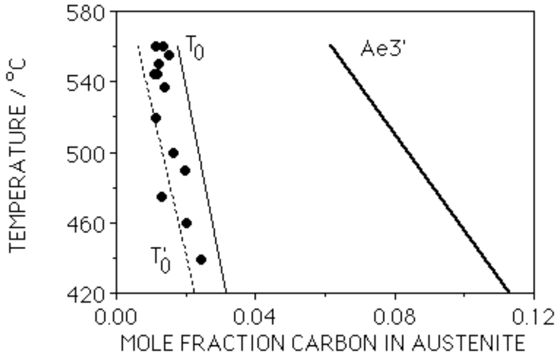

FIGURE 2: Data from experiments in which the austenite is transformed isothermally to acicular ferrite, showing that the reaction stops when the carbon concentration of the austenite reaches the T_0' curve (after Strangwood).

any other feature, causes an immediate change in the microstructure from acicular ferrite to bainite. The same effect can be obtained by increasing the number density of austenite grain nucleation sites relative to intragranular sites. This can be done by refining the austenite grains to obtain a transition from an acicular ferrite microstructure to one which is predominantly bainitic.

The opposite phenomenon, in which an inclusion–containing steel with bainite can be induced to transform into an acicular ferrite microstructure is also observed. This can be done by rendering the austenite grain surfaces ineffective as nucleation sites, either by decorating the boundaries with a thin layer of inert allotriomorphic ferrite, or by adding a small amount of boron (30 p.p.m). The boron segregates to the boundaries, thereby reducing the boundary energy and making them less favourable sites for heterogeneous nucleation. In general, any method which increases the number density of intragranular nucleation sites relative to austenite grain boundary sites will favour the acicular ferrite microstructure.

We have emphasized here the idea that the transformation mechanism for acicular ferrite is identical to that for bainite. However, all phases can nucleate on inclusions, including Widmanstätten ferrite [13,14]. Thewlis *et al.* have argued that in some welds the so–called acicular ferrite may predominantly be intragranularly nucleated Widmanstätten ferrite rather than bainite [15]. They reached this conclusion by noting that the estimated bainite–start (B_S) temperature was lower than that at which coarse plates nucleated on very large inclusions (3–9 μm diameter). Although there is uncertainty in their calculated B_S values, the conclusion that a mixed microstructure of intragranularly nucleated Widmanstätten ferrite and intragranularly nucleated bainite (*i.e.* acicular ferrite) was obtained seems justified. Intragranularly nucleated Widmanstätten ferrite can be distinguished readily from bainite by the scale of the optical microstructure.

Widmanstätten ferrite plates are always much coarser than bainite because what appears as a single plate using optical microscopy is in fact an adjacent pair of self accommodating plates. The shape deformation consists of two adjacent invariant–plane strains which tend to mutually accommodate and hence reduce the strain energy, thus allowing the plates to be coarse [16]. A prediction made here is that transmission electron microscopy should reveal the two components of each of the optically observed plates, with the adjacent variants separated by a low–energy grain boundary [16]. (Note: there is some confusion in [15] where the intragranularly nucleated ferrite plates are identified with reconstructive transformation; in steels, all ferritic phases in the form of plates grow by a displacive mechanism with an accompanying shape deformation characterised by a large shear [12].)

It is the present author's opinion that the weight of evidence supports the conclusion that the acicular ferrite which is recognised to be beneficial to weld metal is in fact intragranularly nucleated bainite. And that the term acicular ferrite should be reserved for such a fine microstructure. If coarse Widmanstätten ferrite forms on inclusions then it can be called "intragranularly nucleated Widmanstätten ferrite". The names given to phases are important because they imply a mechanism of transformation which in turn implies a methodology for the prediction of microstructure. It is particularly important to avoid naming a mixture of microstructures.

4. AUSTENITE FORMATION

The welding process inevitably heats some of the surrounding solid metal into the austenite phase field. It is useful, therefore, to be able to model quantitatively the transformation of an ambient temperature steel microstructure into austenite. This applies both to the weld metal since a gap can be filled with many weld passes, and to the heat affected zone of the steel plate being joined.

The formation of austenite during heating differs in many ways from those transformations that occur during the cooling of austenite. For cooling transformations, the kinetics of decomposition follow the classical C-curve behaviour, in which the rate goes through a maximum as a function of the undercooling below the equilibrium transformation temperature. This is because diffusion becomes sluggish with decreasing temperature, but the driving force for transformation increases with the undercooling. On the other hand, both the diffusion coefficient and the driving force increase with the extent of superheat above the equilibrium temperature, so that the rate of austenite formation must increase indefinitely with temperature, Fig. 3.

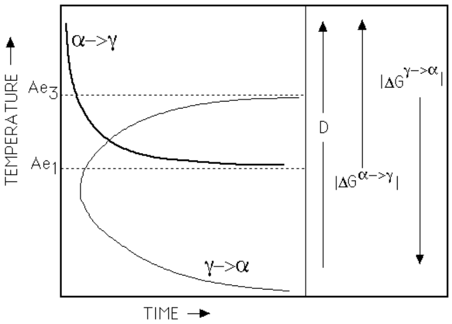

FIGURE 3: The time–temperature–transformation curves for the $\gamma \rightarrow \alpha$ reaction, and for the reverse $\alpha \rightarrow \alpha$ transformation. α and γ represent ferrite and austenite, respectively. ΔG represents the chemical driving force for transformation; D is the rate–controlling diffusion coefficient.

There is another important difference between the transformation of austenite, and the transformation to austenite. In the former case, the kinetics of transformation can be described completely in terms of the alloy composition and the austenite grain size. By contrast, the microstructure from which austenite may grow can be infinitely varied. Many more variables are therefore needed to describe the kinetics of austenite formation. The extent to which the starting microstructure has to be specified remains to be determined, but factors such as particle size, the distribution and chemistry of individual phases, homogeneity, the presence of nonmetallic inclusions, *etc.* should all be important.

This discussion highlights the complexity of the problem. A fundamental attempt at modelling the formation of austenite is therefore unlikely to be of general value, except at slow heating rates consistent with the achievement of equilibrium. Some aspects of the difficulties involved have been reviewed recently for a variety of starting microstructures [12]. Models of specific metallurgical approaches exist for austenite formation from a mixture of cementite and ferrite [17], from bainite [18], and from ferrite [19]. However, none of these are of general applicability for the reasons described earlier.

To resolve this problem, Gavard and co–workers [20] have developed a neural network [21] model to enable the austenite–start (Ac_1) and austenite–finish (Ac_3) temperatures to be estimated as a function of the steel chemical composition and the heating rate. The method involves a non–linear regression of a vast quantity of experimental data. The predictions can then be used to estimate the fraction of austenite (V_γ) that forms at any temperature T [21]:

$$V_\gamma = \frac{1 - \exp\left\{ -k_0 \exp\left\{ \frac{-Q}{kT} \right\} \left[\frac{T - Ac_1}{Ac_3 - Ac_1} \right]^n \right\}}{1 - \exp\{-k_0 \exp(-Q/k\, Ac_3)\}}$$

where $Q/k = 0.12 \times 10^{-6}\,\mathrm{K}$, $k_0 = 0.0206$ and $n = 0.849$ and k is the Boltzmann constant.

This work has not yet been applied to welding but is ready to be incorporated into detailed models on weld metal microstructure.

5. TEMPERING REACTIONS

There is a large range of heat–resistant steels and welding alloys, generally rich in Cr, Mo, V, Nb and W. The ones with the lowest solute concentrations might contain substantial quantities of allotriomorphic ferrite and some pearlite, but the vast majority have bainitic or martensitic microstructures in the normalised condition. After normalising the steels are severely tempered to produce a "stable" microstructure consisting of a variety of alloy carbides in a ferritic matrix. The task is therefore to model the evolution of precipitation and dissolution reactions.

In order to calculate time–temperature–transformation diagrams for carbide reactions, a theory capable of handling several simultaneous precipitation reactions has been developed [23], where the different phases influence each other, for example by drawing the same solute from the matrix ferrite.

In practice, there are many cases where several transformations occur together. The different reactions interfere with each other in a way which is seminal to the development of power plant microstructures. The principles involved are first illustrated with an example in which β and θ precipitate at the same time from the parent phase which is designated α. For the sake of discussion it is assumed that the nucleation and growth rates do not change with time and that the particles grow isotropically.

The increase in the extended volume due to particles nucleated in a time interval $t = \tau$

to $t = \tau + d\tau$ is, therefore, given by

$$dV_\beta^e = \frac{4}{3}\pi G_\beta^3 (t-\tau)^3 I_\beta(V)\ d\tau \qquad \text{and} \qquad dV_\theta^e = \frac{4}{3}\pi G_\theta^3 (t-\tau)^3 I_\theta(V)\ d\tau \tag{1}$$

where G_β, G_θ, I_β and I_θ are the growth and nucleation rates of β and θ respectively, all of which are assumed here to be independent of time. V is the total volume of the system. For each phase, the increase in extended volume will consist of three separate parts. Thus, for β: (i) β which has formed in untransformed α. (ii) β which are formed in regions which are already β. (iii) β which has formed in regions which are already θ.

Only β formed in untransformed α will contribute to the real volume of β. On average a fraction $\left(1 - \frac{V_\beta + V_\theta}{V}\right)$ of the extended volume will be in previously untransformed material. It follows that the increase in real volume of β is given by

$$dV_\beta = \left(1 - \frac{V_\beta + V_\theta}{V}\right) dV_\beta^e \qquad \text{and} \qquad dV_\theta = \left(1 - \frac{V_\beta + V_\theta}{V}\right) dV_\theta^e \tag{2}$$

Generally V_β will be some complicated function of V_θ and it is not possible to integrate these expressions analytically to find the relationship between the real and extended volumes. Numerical integration is straightforward and offers the opportunity to change the boundary conditions for nucleation and growth as transformation proceeds, to account for the change in the matrix composition during the course of reaction. The method can in principle be applied to any number of simultaneous reactions.

The multiple reactions found in power plant steels have important complications which can all be dealt with in the scheme of simultaneous transformations as presented above. The phases interfere with each other not only by reducing the volume available for transformation, but also by removing solute from the matrix and thereby changing its composition. This change in matrix composition affects the growth and nucleation rates of the phases. The main features of the application of the theory to power plant steels are summarised below; a full description is given in references [23,24].

- The model allows for the simultaneous precipitation of M_2X, $M_{23}C_6$, M_7C_3, M_6C and Laves phase. M_3C is assumed to nucleate instantaneously with the paraequilibrium composition. Subsequent enrichment of M_3C as it approaches its equilibrium composition is accounted for.

- All the phases, except M_3C, form close to their equilibrium composition. The driving forces and compositions of the precipitating phases are calculated using MTDATA [25].

- The interaction between the precipitating phases is accounted for by considering the change in the average solute level in the matrix as each phase forms.

- The model does not require prior knowledge of the precipitation sequence.

- Dissolution of non–equilibrium phases is incorporated as a natural event.

- A single set of fitting parameters for the nucleation equations (site densities and surface energies) has been found which is applicable to a wide range of power plant steels.

A plot showing the predicted variation of volume fraction of each precipitate as a function of time at 600 °C is shown in Fig. 4. These results have been shown to be consistent with experiments; the precipitation kinetics of $M_{23}C_6$ are predicted to be much slower in the $2\frac{1}{4}$Cr1Mo steel compared to the 10CrMoV and 3Cr1.5Mo alloys. One contributing factor is that in the $2\frac{1}{4}$Cr1Mo steel a relatively large volume fraction of M_2X and M_7C_3 form prior to $M_{23}C_6$. These deplete the matrix and therefore suppress $M_{23}C_6$ precipitation. The volume fraction of M_2X which forms in the 10CrMoV steel is relatively small, and there remains a considerable excess of solute in the matrix, allowing $M_{23}C_6$ to precipitate rapidly. Similarly, in the 3Cr1.5Mo steel the volume fractions of M_2X and M_7C_3 are insufficient to suppress $M_{23}C_6$ precipitation to the same extent as in the $2\frac{1}{4}$Cr1Mo steel.

$M_{23}C_6$ is frequently observed in the form of coarse particles which are less effective in hindering creep deformation. Delaying its precipitation would have the effect of stabilising the finer dispersions of M_2X and MX to longer times with a possible enhancement of creep strength.

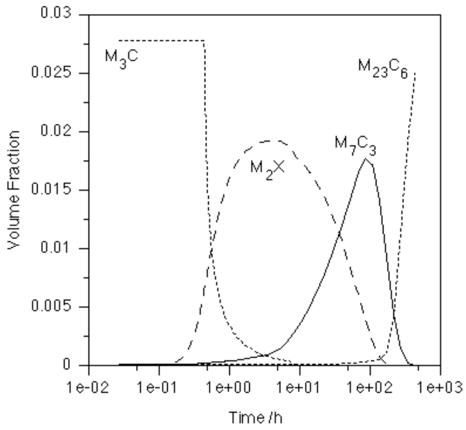

FIGURE 4: The predicted evolution of precipitate volume fractions at 600 °C for $2\frac{1}{4}$Cr1Mo steel [23].

Calculations like these can be used to design microstructures exploiting knowledge built up over decades concerning what is good or bad for creep strength. It is often argued that Laves phase formation is bad for creep resistance – it leads to a reduction in the concentration of solid solution strengthening elements; since the Laves precipitates are few and coarse, they do not themselves contribute significantly to strength. The model presented here can be used to design against Laves phase formation.

6. CONCLUSIONS

It is impossible in a short paper such as this to do justice to the progress that has been made on the modelling of weld metal microstructures. The references listed in this paper are much better reviews in this respect. The latest issues, which have been the focus of this paper, show that there is continued progress with aspects of basic science grappling with some of the most complex technology. What could possibly be a more exciting research topic for metallurgists?

REFERENCES

[1] Alberry, P. J. and Jones, W. K. C., Metals Technology 9, (1982) pp. 419–427.

[2] Ashby, M. F. and Easterling, K. E., Acta Metallurgica 30, (1982) 1969–1978.

[3] Bhadeshia, H. K. D. H., Materials Science and Technology 8, pp. 123–133 (1992).

[4] Bhadeshia, H. K. D. H. and Svensson, L–E., Mathematical Modelling of Weld Phenomena, eds H. Cerjak and K. E. Easterling, The Institute of Materials, London, 1993, pp. 109–182.

[5] Svensson, L.–E., Control of Microstructure and Properties in Steel Arc Welds, London, CRC Press, 1993.

[6] Zacharia, T., Vitek, J. M., Goldak, J. A., Debroy, T. A., Rappaz M. and Bhadeshia, H. K. D. H., Modelling and Simulation in Materials Science and Engineering, 3, pp. 265–288 (1995).

[7] Bhadeshia, H. K. D. H., Mathematical Modelling of Weld Phenomena II, eds H. Cerjak and H. K. D. H. Bhadeshia, The Institute of Materials, London, 1995, pp. 71–118.

[8] Grong, O., Metallurgical Modelling of Welding, 2nd edition, London, Institute of Materials, 1997.

[9] Christian, J. W., Acta Metallurgica 6, pp. 377-379 (1958).

[10] Hillert, M., Jernknotorets Ann. 135 p.403 (1951).

[11] Chandrasekharaiah, M. N., Dubben, G. and Kolster, B. H., Welding Journal, 71 pp. 247s-252s (1994).

[12] Bhadeshia, H. K. D. H., Bainite in Steels, The Institute of Materials, London, 1992.

[13] Dubé, C. A., Ph.D. Thesis, Canegie Institute of Technology, (1948).

[14] Ali, A. and Bhadeshia, H. K. D. H., Materials Science and Technology, 7, pp. 895–903 (1991).

[15] Thewlis, G., Whiteman, J. A. and Senogles, D. J., Materials Science and Technology 13, pp. 257–274 (1997).

[16] Bhadeshia, H. K. D. H., Acta Metallurgica, 29, pp. 1117–1130 (1981).

[17] Hillert, M., Nilsson, K. and Torndahl, L-E. JISI, 209, pp. 49–66, (1971).

[18] Yang, J. R. and Bhadeshia, H. K. D. H, Materials Science and Engineering A, A118, pp. 155–170 (1989).

[19] Atkinson, C., Akbay, T. and Reed, R. C., Acta Metallurgica et Materialia, 43, pp. 2013–2031 (1995).

[20] Gavard, L., Bhadeshia, H. K. D. H., MacKay, D. J. C. and Suzuki, S., Materials Science and Technology 12 pp. 453–463 (1996).

[21] MacKay, D. J. C., Neural Computation, 4, pp. 415–447 (1992).

[22] Chester, N. and Bhadeshia, H. K. D. H., unpublished work, University of Cambridge, 1998.

[23] Robson, J. D. and Bhadeshia, H. K. D. H., Materials Science and Technology, 13, pp. 631–644, 1997.

[24] Robson, J. D. and Bhadeshia, H. K. D. H., Calphad, 20, pp. 447-460 (1996).

[25] MTDATA, Metallurgical and Thermochemistry Group, National Physical Laboratory, Teddington, 1998.